Peer-reviewed version available at *Molecules* **2020**, *25*, 439; doi:10.3390/molecules25030439

Article

Poly(Vinyl Butyral-co-Vinyl Alcohol-co-Vinyl Acetate) Coating Performance on Copper Corrosion in Saline Environment

Adriana Samide [1], Claudia Merisanu [1,2], Bogdan Tutunaru [1]* and Gabriela Eugenia Iacobescu [3]

[1] University of Craiova, Faculty of Sciences, Department of Chemistry, 107i Calea Bucuresti, Craiova, Romania; samide_adriana@yahoo.com
[2] University of Craiova, Faculty of Sciences, Doctoral School of Sciences, A.I. Cuza no.13, Craiova, Romania; claudia.merisanu@yahoo.com
[3] University of Craiova, Faculty of Sciences, Department of Physics, A.I. Cuza no.13, Craiova, Romania; gabrielaiacobescu@yahoo.com
* Correspondence: tutunaruchim@yahoo.com ; University of Craiova, Faculty of Sciences, Department of Chemistry, CUI: 4553380, 107i Calea Bucureşti, Craiova, Romania, Tel/Fax: +040251-597048

Abstract: Poly(vinyl butyral-co-vinyl alcohol-co-vinyl acetate) named further PVBA was investigated as protective coating for copper corrosion in 0.9 % NaCl solution using electrochemical measurements such as, electrochemical impedance spectroscopy (EIS) and potentiodynamic polarization associated with Atomic Force Microscopy (AFM). The PVBA coating on the copper surface (Cu-PVBA) was modeled in methanol containing PVBA. Its inhibitory properties against corrosion was comparatively discussed with those of the copper sample treated in methanol without polymer (Cu-Me) and of untreated sample (standard copper). A protective performance of PVBA coating of 80 % was computed from electrochemical measurements, for copper corrosion in NaCl solution. Also, AFM images designed a specific surface morphology of coated surface with PVBA, clearly highlighting a polymer film adsorbed on the copper surface, which presents certain deterioration after corrosion, but metal surface was not significantly affected compared to those of untreated samples or treated in methanol, in the absence of PVBA.

Keywords: adsorption; coatings; Poly(vinyl butyral-co-vinyl alcohol-co-vinyl acetate); corrosion tests; Atomic Force Microscopy.

1. Introduction

Corrosion control of metals/alloys, as well as the choice of corrosion inhibitors are important issues facing certain industrial fields. Production, synthesis and transportation of corrosive products lead to the failure of metallic materials resulting in environmental and economic problems. Certain corrosion protection strategies take into consideration assembling of some surface coatings using the inorganic and organic polymers with inhibitory properties and low costs, thus retarding the destructive effects caused by the metal oxidation processes [1-3].

In this regard, eco-friendly, natural and synthetic polymers were successfully used to protect different metallic substrates against corrosion [1-4].

An effective material for corrosion protection of 2024–T3 aluminum alloy [5] was obtained by encapsulating of some organic inhibitor molecules in polylactic acid/polysiloxane hybrid nanoparticles. An epoxy resin polymer with aluminum oxide insertions having a self-regeneration ability was tested for aluminum corrosion protective coating [6].

Graphene and graphene/epoxy ester-siloxane-urea hybrid polymer nanocomposite were tested by potentiodynamic polarization and electrochemical impedance spectroscopy to determine the

corrosion resistance of coated aluminum alloy [7,8]. Also, graphene oxide functionalized with acrylamide/acrylic acid copolymer provided a good corrosion protection for the magnesium alloy surface [9]. Moreover, by potentiodynamic polarization and electrochemical impedance spectroscopy, high value of coating protection efficiency of 99.8 % was computed. On the other hand, biodegradable magnesium alloys have been coated with polymeric thin films (polyamide, polyacrylic acid, polylactic acid, polydopamine, chitosan, collagen, poly(lactic-co-glycolic)acid, polycaprolactone, enhancing their corrosion resistance [10-12].

Special attention was paid to steel corrosion processes and implicitly to its protection with polymeric films. The environmentally polymers with self-regeneration properties were studied to improve the corrosion resistance by their adsorption on the steel surface [13-16].

The copolymers represent a specific class of polymers, which also were used for coating modeling at metal-environment interface to obstruct the corrosion [17-20].

The copolymer as poly(maleic anhydride-co-N-vinyl-2-pyrrolidone), poly(3,4-ethylenedioxythiophene-co-indole-5-carboxylic acid), poly(methyl methacrylate-co-N-vinyl-2-pyrrolidone) and polyaniline/polystyrene/polybutadiene were reported as effective corrosion inhibitors [17-20]. The electrochemical measurements, UV-Vis spectroscopy, X-ray diffraction, X-ray photoelectron spectroscopy, scanning electron microscopy, Raman and Fourier-transform infrared spectroscopy and thermogravimetric analysis were employed to investigate the composition and efficiency of polymer films adsorbed under various conditions and changing the steel surface features [21-27].

Copper has many applications in various field due to its mechanical and electrical properties. Despite its good properties, copper is susceptible to corrosion in the presence of chloride ions. Polymer coatings such as polyamide, chitosan, polycarvacrol and polythymol provide effective anticorrosion layers for copper surface [28-30].

Polymer networks based on vinyl butyral units presents interesting property as the “shape memory” [31,32], having the ability to recover the initial shape upon exposure to an external thermal, chemical, magnetic, mechanical or electrical stimulus [33]. The multi-functional shape memory polymers possess also self-regeneration, anticorrosion, drug delivery or other properties [33,34]. The polymers based on poly(vinyl butyral) have many applications, including the manufacturing of some materials for automotive safety glasses, encapsulation of solar modules, or as a binder for different coatings, adhesives, paintings, enamels and inks. The functional groups from macromolecular chain are responsible for its adsorption properties on various materials through covalent and/or hydrogen bonding.

In the current study, the PVBA film protective performance against copper corrosion in saline environment was investigated by electrochemical impedance spectroscopy (EIS), potentiodynamic polarization and atomic force microscopy (AFM). Three types of copper samples were studied, as follows: (1) standard copper; (2) copper treated in methanol without polymer denoted as (Cu-Me); (3) copper treated in methanol containing copolymer named further PVBA (Cu-PVBA).

2. Results and discussion

2.1. Open circuit potential discussion

The potential variation at open circuit was recorded, as shown in Figure 1. A similar behavior is observed of the Cu-Me sample with the standard one (curves 1 and 2), meaning that a slowly potential decrease over time takes place, with a stabilization tendency in respect with an exponential function.

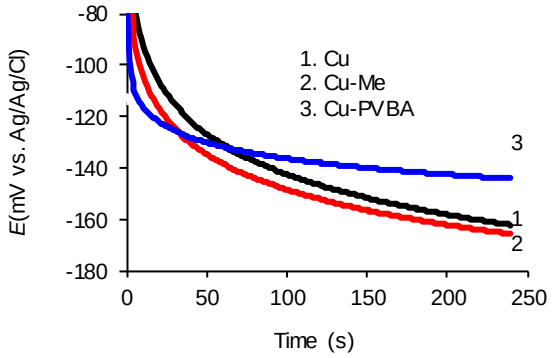

Figure 1. Variation of the open-circuit potential for standard copper, methanol-treated copper and PVBA modified copper, recorded in 0.9 % NaCl solution.

In contrast, in the presence of PVBA (Cu-PVBA sample) in NaCl solution, the open circuit potential stabilizes, after 60 sec., around the value of -148 mV. This is higher by about 20 mV than those of the standard copper and Cu-Me samples, indicating that the surface characteristics were changed due to PVBA adsorbed on the surface leading to the restriction of the ion exchange at the metal/electrolyte interface.

2.2. Electrochemical impedance spectroscopy (EIS)

As shown in Figure 2, classical Nyquist diagrams (Fig. 2a) were obtained for all three samples immersed in sodium chloride solution, highlighting capacitive loops with approximately semicircular shapes whose diameter gradually increases, reaching the highest value for Cu-PVBA sample.

The Bode diagram (Fig. 2b) designs for impedance, almost overlapped curves for standard copper and the one treated in methanol and a completely distinct one for Cu-PVBA, having the highest response in the low frequency area, respectively at 0.1 Hz. The Bode impedance curves indicate that the copolymer macromolecules were adsorbed on the metal surface, modeling a surface film that leads to the increase of copper impedance response (Z) and by default the charge transfer resistance (R_{ct}) [35-38], the results being in good agreement with those observed from Nyquist diagram. On the other hand, the phase Bode diagram shows that: (i) the standard copper forms a maximum of the phase angle at -46.3 degrees, generating a small loop followed by an uncertain sholder with a wide maximum located at -44.5 degrees that slowly increases until 0.1 Hz; (ii) a large phase angle maximum around -48.8 degrees was formed in the case of Cu-Me sample exhibited in NaCl solution which gradually decreases in the area of very low frequencies, indicating a slightly different behavior from that of the standard copper due to the chemically finished of the metallic surface with methanol; (iii) a completely distinct curve was recorded for Cu-PVBA having a phase angle well-contoured maximum at -57.1 degrees, indicating a different chemical composition of the upper layer [38] due to the PVBA macromolecules adsorbed on the surface, which drastically changes the metal behavior to corrosion.

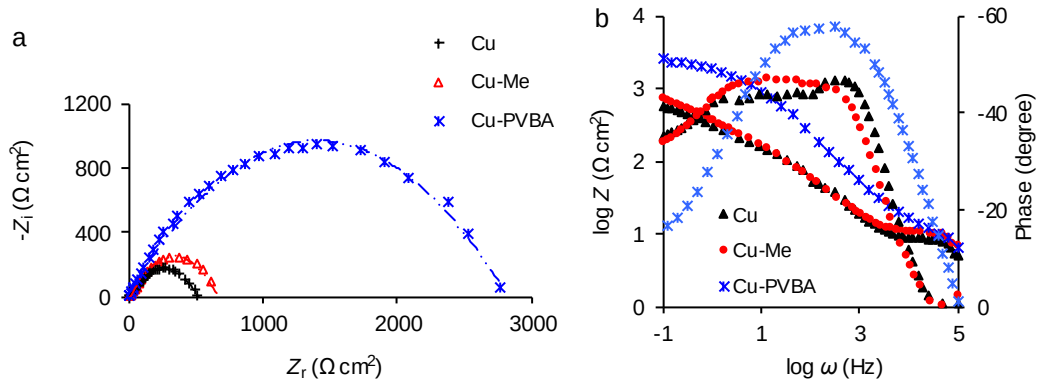

Figure 2. Nyquist (a) and Bode (b) diagrams for standard copper, methanol-treated copper (Cu-Me) and PVBA modified copper (Cu-PVBA) recorded in 0.9 % NaCl solution.

The determination of the electrochemical parameters from EIS was performed by fitting the experimental data according to a simple circuit consisting of three elements, as: charge transfer resistance (R_{ct}) connected in a parallel position with the double-layer capacitance (C_{dl}), both linked in series with the solution resistance (R_s). The coating protection performance (P%) was computed from both equations 1 and 2 [39]. The results are listed in Table 1.

$$P\% = \left(1 - \frac{Z^S}{Z_{PVBA}}\right) x100 \quad (1)$$

where Z_s is the impedance response in the PVBA coating absence and Z_{PVBA} represents the impedance response in the presence of PVBA adsorbed coating on the copper surface.

$$P\% = \frac{R_{ct}^{PVBA} - R_{ct}^{S}}{R_{ct}^{PVBA}} x100 \quad (2)$$

where R_{ct}^{S} is the charge transfer resistance of standard sample and R_{ct}^{PVBA} represents the charge transfer resistance of Cu-PVBA sample.

Table 1. Electrochemical parameters calculated from electrochemical impedance spectroscopy recorded at room temperature in 0.9 % NaCl solution for standard copper, methanol-treated copper and PVBA modified copper.

Sample	E_{OCP} (mV vs. AgAgCl	R_s (Ω cm²)	R_{ct} (Ω cm²)	C_{dl} (μF cm⁻²)	log | Z | (Ω cm²)	Z (Ω cm²)	Angle phase max (degree)	P (%)
Standard	-164	245	515	845	2.71	513	-46.3/defined -44.5/broad	-
Cu-Me	-167	132	650	612	2.84	692	-48.8/broad	-
Cu-PVBA	-147	64	2763	342	3.43	2692	-57.1/well defined	80.9

Analyzing the data from the Table 1, it can be observed that there is a good correlation between the impedance responses and the charge transfer resistance, their highest values being obtained in the case of Cu-PVBA sample, when the lowest values were recorded for C_{dl} and R_s.

PVBA film protection performance reached a value of about 81.0 % calculated from both equations, 1 and 2, mentioned above.

2.3. Potentiodynamic polarization

After EIS, the potentiodynamic polarization was applied on the three electrodes namely standard copper (Cu), methanol treated copper (Cu-Me) and PVBA modified copper (Cu-PVBA) registering both diagrams (Fig. 3), the semilogarithmic (Fig. 3a) and the linear one (Fig. 3b).

As shown in Fig. 3a, the Cu-Me sample similarly behaves to the standard one. The potentiodynamic curves are framed within the same potential range and current area, which led to their apparent overlap, with a slight displacement of the one corresponding to Cu-Me towards lower current area. The presence of PVBA molecules adsorbed on the copper surface leads to the shifting of potentiodynamic curves to negative direction and lower current area compared to those discussed above. Consequently, the polymer coating adsorbed on the copper surface leads to the corrosion current decrease and polarization resistance increase as it is demonstrated from linear diagram (Fig. 3b) recorded in the potential range (±20 mV) close to corrosion potential (E_{corr}). The corrosion current density (i_{corr}) was computed at Tafel lines intersection extrapolated towards corrosion potential, the best fitting of potentiodynamic data being in the potential range of ±250 mV, in respect with E_{corr}. The anodic and cathodic Tafel slopes were determined with a mean squared deviation, R^2 of 0.99.

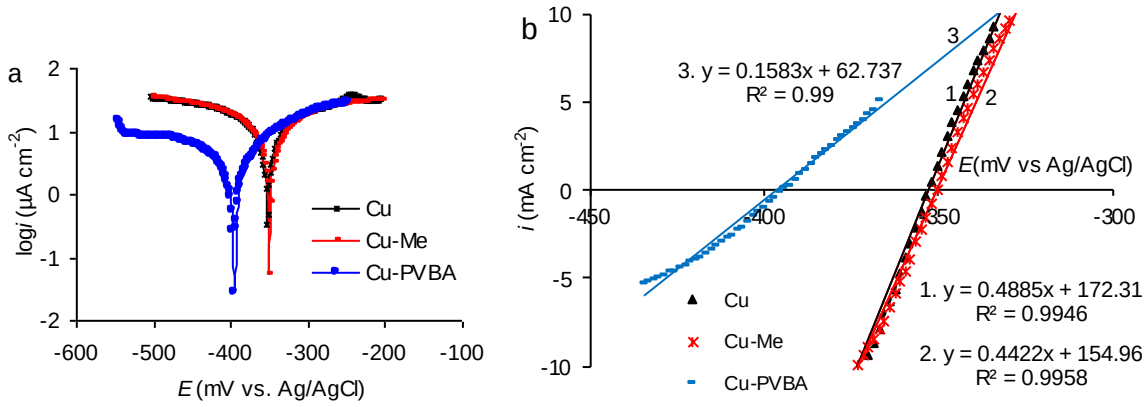

Figure 3. Potentiodynamic polarization curves recorded with a potential scan rate of 1.0 mV s^{-1}, on standard copper, methanol-treated copper and PVBA modified copper, in 0.9 % NaCl solution, at room temperature: a - semilogarithmic curves; b - linear diagram drawn in the potential range close to corrosion potential (±20 mV).

By deriving the equations inserted in Fig. 3b, the slope of the straight lines drawn as tangents to the polarization curves recorded in a potential range close to the corrosion potential was computed [37,40]. Thus, the polarization conductance (C_p) was determined from the corresponding line slope (di/dE) [37,40] and implicitly the polarization resistance (R_p) was deduced as $1/C_p$ [37,40]. The electrochemical parameters are shown in Table 2.

Table 2. The electrochemical parameters calculated from potentiodynamic measurements for standard Cu, methanol-treated Cu and PVBA modified Cu, in 0.9 % NaCl solution, at room temperature.

Sample	E_{corr} (mV vs. Ag/AgCl)	i_{corr} (μA cm^{-2})	b_a (mV dec^{-1})	b_c (mV dec^{-1})	$C_p 10^3$ (mS cm^{-2})	R_p (Ω cm^2)	P (%)
Standard	-353	10.2	179	-172	0.4885	2047	-
Cu-Me	-350	11.3	228	-232	0.4422	2261	-
Cu-PVBA	-395	2.03	133	-260	0.1583	6317	80.1

Analyzing the values of the electrochemical parameters, it was found that the methyl alcohol does not have a protective effect on the copper surface, but rather represents a degreasing agent and consequently, the corrosion current computed for Cu-Me maintained at approximately the same value as in the standard case. The polarization resistance of the Cu-PVBA sample increases significantly compared to both standard and Cu-Me samples, indicating that the polymer layer is stable and adherent on the copper surface. The layer protection performance (P%) calculated with Eq. 3, has maintained at a high level, very close to the one calculated from the EIS, meaning that during the impedance measurements, very limited desorption process of PVBA took place and consequently, the polymer molecules are strongly linked from copper substrate.

$$P\% = \frac{i_{corr}^{S} - i_{corr}^{PVBA}}{i_{corr}^{S}} x100 \quad (3)$$

where i_{corr}^{S} is the corrosion current density of standard sample and i_{corr}^{PVBA} represents the corrosion current density of Cu-PVBA sample, respectively.

Thus, it can be certainty stated that the PVBA molecules are strongly adsorbed on the substrate through numerous adsorption centers existing along the macromolecular chain such as oxygen atoms.

2.4. PVBA adsorption mechanism

Analyzing the PVBA molecular formula (Fig. 4), three distinct structural units are observed, as follows [42]: the hydrophobic groups (in a highest proportion) corresponding to the polyvinyl butyral macromolecular chain; hydrophilic groups from polyvinyl alcohol; in a smaller proportion, the acetate groups from polyvinyl acetate.

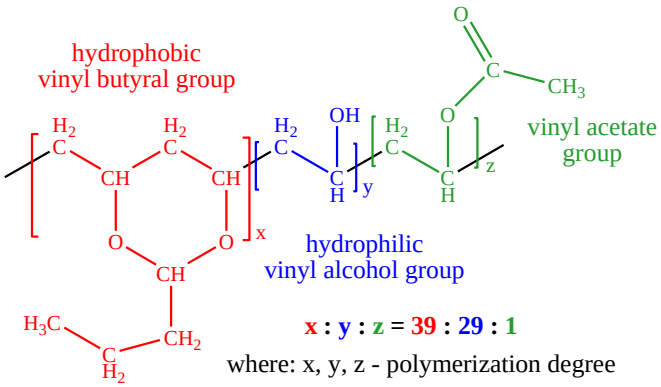

Figure 4. Molecular structure of poly(vinyl butyral-co-vinyl alcohol-co-vinyl acetate).

In context with the polar and nonpolar character of the mentioned groups, PVBA has adhesive properties with different materials such as glass, metals and wood [32] through "hydrogen bonds (noncovalent interactions), metal coordination, host-guest interactions, ionic attractions, hydrophobic interactions" as shown by Zhi-Chao Jiang et al. in a previous study [33]. The hydroxyl groups enable the PVBA outstanding adhesion to many substrates including the metal surfaces (aluminum, brass, tin, lead, iron) increasing moisture resistance [42]. PVBA good binding capacity on copper surface and resistance to aqueous NaCl solution are proved by the open circuit measurements (Fig. 1) which show that Cu-PVBA sample potential was stabilized to higher value compared to those of standard and Cu-Me samples, when the open circuit potential stabilization is relative being observed a slightly descending trend. Copper has a good ability for methanol adsorption [43], but its low resistance at the NaCl solution can favor desorption of the molecules, which leads to an electrochemical behavior close to the one of standard (Figs. 2 and 3).

When a perturbation appears on Cu-PVBA sample, such as frequency variation during impedance spectroscopy, the PVBA coating ensures a significant copper surface protection in sodium chloride solution, probably due to the polymer ability to return at its predetermined shape from a temporary one, as response to the external stimulus, providing the characteristics of a shape memory polymer, as PVBA was described [31].

Consequently, by the simple dipping method of the copper sample in methanol containing PVBA the adsorption process involves two stage: (1) initially, the adsorption of the methyl alcohol molecules on the copper surface takes place, prevailing on that of macromolecules due to steric arrangement of the polymeric chain, imposing a more restricted diffusion towards the interface; consequently, noncovalent interactions as hydrogen-bridged between hydroxyl groups from adsorbed methanol and hydroxyl groups from polyvinyl macromolecular chain can occur; (2) the hydrophobic interactions due to vinyl butyral groups represents the most likely adsorption process of PVBA macromolecules on the copper surface supplemented by a host-guest adsorption in which the copper metal network constitutes the matrix incorporating the polymer.

After the potentiodynamic polarization, the PVBA layer protection performance maintained at a similar value to that calculated from the EIS. Thus, the layer stability is preserved, the desorption of the polymer on the copper surface does not occur to an extent that affects the PVBA protective performance.

In this regard, some additional explanations are necessary. During potentiodynamic polarization, copper oxidation processes take place on the polymer-free areas. The copper ions favor the polyvinyl alcohol crosslinking reaction [39] and formation of some copper (I and II) complexes [39] which coordinatively binds on the metal surface, leading to the change of its characteristics and morphology, without affecting the polymer coating protective performance.

2.5. Atomic Force Microscopy

AFM 2D and 3D images were acquired before the electrochemical measurements and after potentiodynamic polarization, in order to observe the morphological characteristics of the copper surface coated with PVBA compared to those of the standard (Cu) and copper immersed in methanol (Cu-Me). Figure 5 shows the AFM slides designed before the electrochemical measurements.

Thus, three different morphological characteristics of the copper surface can be observed, namely: (i) for standard copper the AFM 2D and 3D images displays a surface morphology corresponding to a mechanically processed surface (Fig. 5a); (ii) the plate immersed in methanol (Cu-Me sample) preserves quite well the characteristics of the standard, however, highlighting more even surface due to the methanol adsorption (Fig. 5b); (iii) the polymer film adsorbed on the copper surface is well nuanced in Fig. 5c which show a morphology completely distinct from those discussed previously, being determined by the change in both characteristics and surface chemistry.

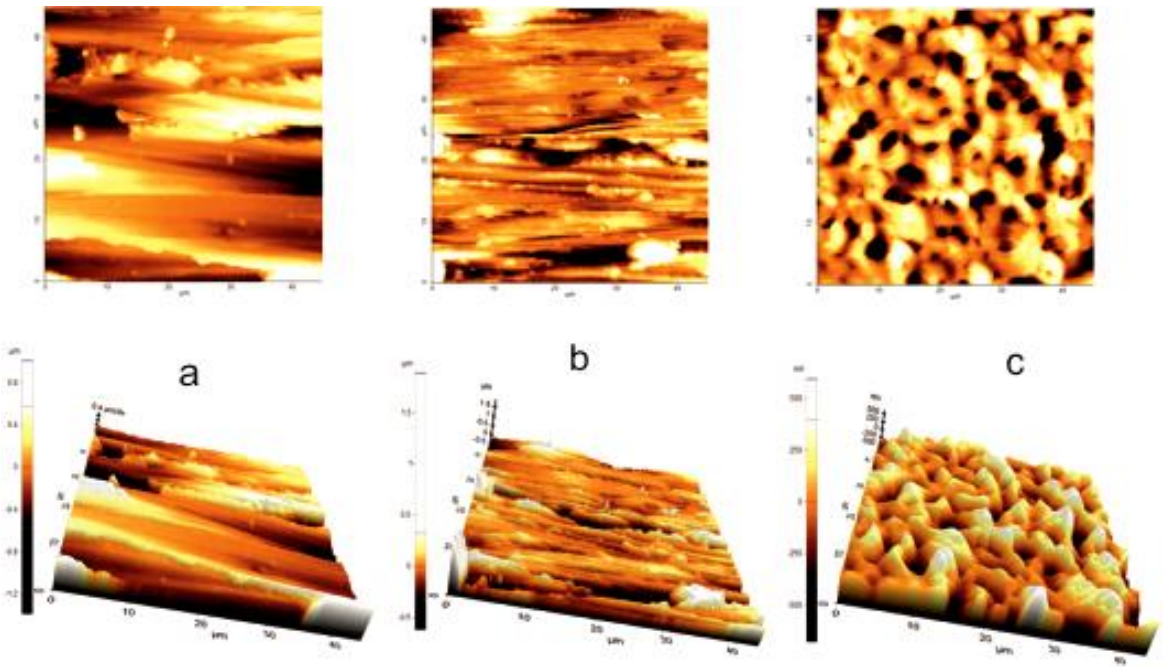

Figure 5. AFM 2D and 3D images obtained for copper surface before electrochemical measurements: a – standard copper; b – copper immersed in methanol (Cu-Me sample); c – copper immersed in methanol containing PVBA (Cu-PVBA sample).

The relatively coherent network appearance organized on the surface clearly differentiates the Cu-PVBA sample from those of the standard or treated in methanol, which demonstrates the adsorption of the polymer on the copper surface. There is virtually no similarity to the standard or the Cu-Me sample.

Figure 6 shows the AFM 2D and 3D images after the potentiodynamic polarization of the samples in 0.9 % NaCl solution. In all cases, the surface appearance has changed compared to that before corrosion.

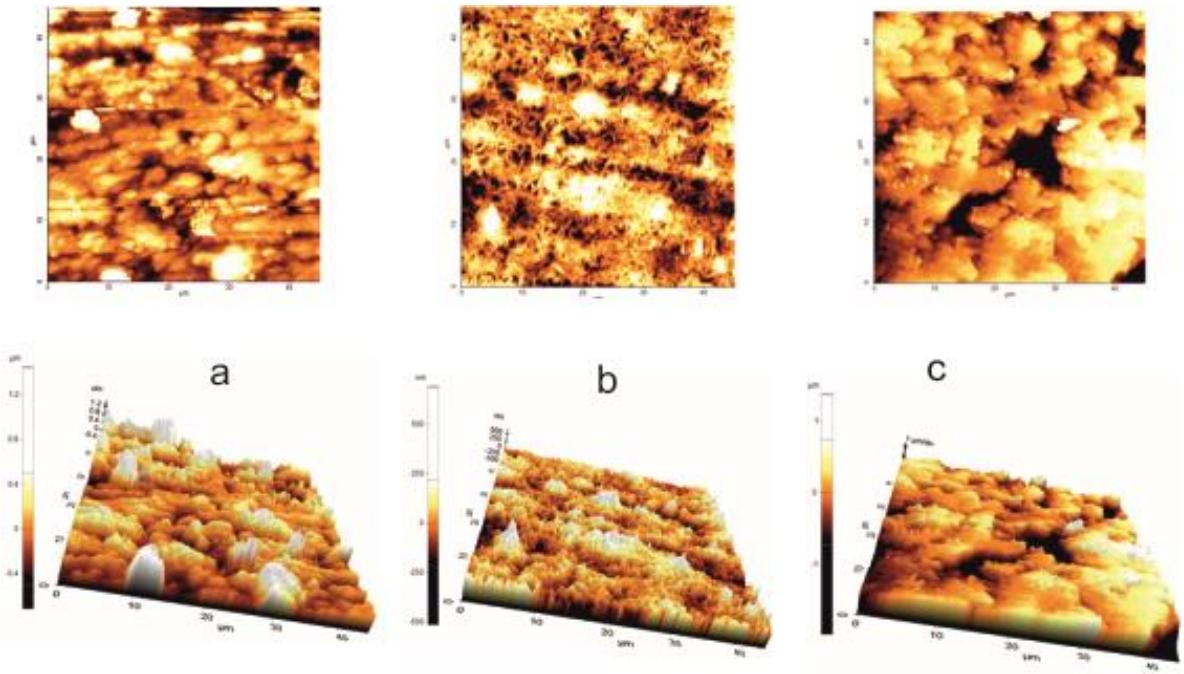

Figure 6. AFM 2D and 3D images obtained for copper surface after potentiodynamic polarization: a – standard copper; b – copper immersed in methanol (Cu-Me sample); c – copper immersed in methanol containing PVBA (Cu-PVBA sample).

Fig. 6a shows that the standard surface has deteriorated as a result of the saline solution corrosive attack. In the case of the sample treated with methanol (Fig. 6b), deposits of smaller sizes occur on the surface compared to those formed on the standard (Fig. 6b), probably due to the adsorbed methanol that inhibits the agglomeration of the corrosion products, reducing the risk of the appearance of large aggregates. Surface morphology from Fig. 6c shows that the polymer film did not desorb on the copper surface. Possible differences from the one shown in Fig. 5c (before corrosion) probably occurs due to the swelling of the absorbed polymer leading to apparently thicker film development. The change in coating texture can be caused by the adsorption of the crosslinked polymer and the copper-PVBA complexes which were formed during the potentiodynamic polarization, as mentioned in the previous paragraph.

3. Materials and methods

3.1. Materials

The copper plates with the area of 2 cm^2 (dimensions: 1 cm x 2 cm) were cut from a copper foil (99.9 % purity) purchased from Sigma Aldrich. Other reagents as methyl alcohol, natrium chloride and poly(vinyl butyral-co-vinyl alcohol-co-vinyl acetate) further named as PVBA were also obtained from Sigma Aldrich. The PVBA composition (wt. %) consists of acetate/hydroxyl/vinyl butyral, in ratio of 1/11/88, its average molecular mass locating between 90000 and 120000.

3.1.1. PVBA coating modeling

Copper plates were polished with sandpaper of different sizes, ultrasonically cleaned, degreased with acetone and dried in warm air referred to as standard copper. After processing, the samples were immersed in methanol without and with PVBA in concentration of 6 %, for 24 hours, at room temperature. The samples were removed from the methanol baths and dried, time of 24 hours, at room temperature and 2 hours in warm air.

Copper samples immersed in methanol (methanol treated copper) will be referred to as Cu-Me, while the copper samples dipped in methanol containing PVBA (PVBA modified copper) will be further denoted to as Cu-PVBA. Thus, three class of copper samples were prepared to be submitted at corrosion in 0.9 % NaCl solution and to be comparatively discussed namely, standard copper (Cu), methanol treated copper (Cu-Me) and PVBA modified copper (Cu-PVBA).

3.2. Corrosion tests

The corrosion behavior of copper samples above mentioned was investigated using electrochemical measurements as the open circuit potential (OCP) variation over time, electrochemical impedance spectroscopy (EIS) and potentiodynamic polarization. Atomic force microscopy (AFM) was performed to examine the changes in surface morphology.

3.2.1. Electrochemical measurements

Electrochemical impedance spectroscopy (EIS) was carried out in 0.9 % NaCl solution, at sample corresponding OCP, in the frequency range of 10^5 Hz and 10^{-1} Hz, with a sinusoidal perturbation, AC signal of 10 mV.

Potentiodynamic polarization was performed in 0.9 % NaCl solution, at room temperature, in the potential range between -1000 mV and 1000 mV, with potential scan rate of 1 mV s^{-1}. The standard electrochemical cell with three electrodes of 100 mL volume was used. The working electrode manufactured from copper, with an active area of 1 cm^2, a platinum auxiliary electrode and Ag/AgCl reference electrode were coupled to an electrochemical system type VoltaLab with VoltaMaster 4 software. The polarization curves were processed as Tafel diagram from which the

corrosion current density (i_{corr}) were computed at the intersection of Tafel lines towards extrapolated to corrosion potential (E_{corr}). Also, the linear diagram was recorded, in the potential range close to corrosion potential (± 20 mV) and the polarization resistance (R_p) was calculated. The experimental method and equipment were reported in our previous studies [35-41].

3.2.2. Atomic Force Microscopy (AFM)

Atomic Force Microscopy was performed as in our previous studies [37, 40, 41], using a non-contact mode atomic force microscopy (NC-AFM, Park Systems, Suwon, Korea), PARK XE-100 SPM system). The cantilever had a nominal length of 125 mm, a nominal force constant of 40 N m^{-1}, and oscillation frequencies in the range of 275–373 kHz. We used horizontal line by line flattening as the planarization method.

The AFM 2D and 3D images were designed for: (i) standard copper surface; (ii) the copper plates immersed in methanol (Cu-Me sample), before and after corrosion; (iii) the copper samples immersed in methanol containing PVBA (Cu-PVBA sample), before and after corrosion.

4. Conclusions

PVBA was chemically deposited on the copper surface using simple dipping method of metal sample in methanol containing dissolved polymer in concentration of 6 %.

The protective performance of PVBA coating on copper corrosion in 0.9 % NaCl solution was investigated by electrochemical measurements such as, the open circuit potential variation, electrochemical impedance spectroscopy (EIS) and potentiodynamic polarization. The surface morphology was examined on atomic force microscopy (AFM) slides acquired before and after corrosion. The PVBA adsorption mechanism on the copper surface was also proposed.

The PVBA protective performance reached a value about of 81 % computed from both EIS and potentiodynamic polarization.

PVBA acted by adsorption on copper surface involving noncovalent interactions between methanol hydroxyl groups and polyvinyl alcohol hydroxyl groups and hydrophobic interactions due to vinyl butyral groups, the metallic network being a good matrix incorporating polymer macromolecules. Moreover, during potentiodynamic polarization, crosslinked polymer and copper-PVBA complexes can be occur, having a good adsorption ability on the metal substrate.

AFM reproduced before and after corrosion a different morphology of the filmed surface compared to those of the standard and treated copper in methanol, indicating that the PVBA coating is stable and good preserved after corrosion.

Author Contributions: Conceptualization, Adriana Samide; Investigation, Claudia Merisanu and Gabriela Eugenia Iacobescu; Methodology, Adriana Samide; Project administration, Adriana Samide; Supervision, Adriana Samide; Writing – original draft, Adriana Samide, Tutunaru Bogdan and Gabriela Eugenia Iacobescu; Writing – review & editing, Claudia Merisanu and Tutunaru Bogdan.

Conflicts of Interest: The authors declare no conflict of interest

Abbreviations

poly(vinyl butyral-co-vinyl alcohol-co-vinyl acetate)	PVBA
copper treated in methanol in the absence of PVBA	Cu-Me
copper treated in methanol in the presence of PVBA	Cu-PVBA
electrochemical impedance spectroscopy	EIS
Atomic Force Microscopy	AFM
open circuit potential	OCP
corrosion current density	i_{corr}

corrosion potential	E_{corr}
polarization resistance	R_p
charge transfer resistance	R_{ct}
double-layer capacitance	C_{dl}
solution resistance	R_s
coating protection performance	P%
polarization conductance	C_p

References

1. Obot, I.B.; Solomon, M.M.; Umoren, S.A.; Suleiman, R.; Elanany, M.; Alanazi, N.M.; Sorour, A.A. Progress in the development of sour corrosion inhibitors: Past, present, and future perspectives. *J. Ind. Eng. Chem.* **2019**, *79*, 1-18.
2. Tiu, B.D.B.; Advincula, R.C. Polymeric corrosion inhibitors for the oil and gas industry: Design principles and mechanism. *React. Funct. Polym.* **2015**, *95*, 25-45.
3. Umoren, S.A.; Eduok, U.M. Application of carbohydrate polymers as corrosion inhibitors for metal substrates in different media: A review. *Carbohyd. Polym.* **2016**, *140*, 314-341.
4. Umoren, S.A.; Solomon, M.M. Protective polymeric films for industrial substrates: A critical review on past and recent applications with conducting polymers and polymer composites/nanocomposites. *Prog. Mater. Sci.* **2019**, *104*, 380-450.
5. Alrashed, M.M.; Jana, S.; Soucek, M.D. Corrosion performance of polyurethane hybrid coatings with encapsulated inhibitor. *Prog. Org. Coat.* **2019**, *130*, 235-243.
6. Yabuki, A.; Nagayama, Y.; Fathona, I.W. Porous anodic oxide film with self-healing ability for corrosion protection of aluminum. *Electrochim Acta* **2019**, *296*, 662-668.
7. Okafor, P.A.; Singh-Beemat, J.; Iroh, J.O. Thermomechanical and corrosion inhibition properties of graphene/epoxy ester–siloxane–urea hybrid polymer nanocomposites. *Prog. Org. Coat.* **2015**, *88*, 237-244.
8. Othman, N.H.; Ismail, M.C.; Mustapha, M.; Sallih, N.; Kee, K.E.; Jaal, R.A. Graphene-based polymer nanocomposites as barrier coatings for corrosion protection. *Prog. Org. Coat.* **2019**, *135*, 82-99.
9. Jin, T.; Xie, Z.; Fullston, D.; Huang, C.; Zeng, R.; Bai, R. Corrosion resistance of copolymerization of acrylamide and acrylic acid grafted graphene oxide composite coating on magnesium alloy. *Prog. Org. Coat.* **2019**, *136*, 105222.
10. Li, L.Y.; Cui, L.Y.; Zeng, R.C.; Li, S.Q.; Chen, X.B.; Zheng, Y.; Kannan, M.B. Advances in functionalized polymer coatings on biodegradable magnesium alloys – A review. *Acta. Biomater.* **2018**, *79*, 23-36.
11. Bertuola, M.; Miñán, A.; Grillo, C.A.; Cortizo, M.C.; Fernández Lorenzo de Mele, M.A. Corrosion protection of AZ31 alloy and constrained bacterial adhesion mediated by a polymeric coating obtained from a phytocompound. *Colloids Surf. B: Biointerfaces* **2018**, *172*, 187-196.
12. Xu, W.; Yagoshi, K.; Koga, Y.; Sasaki, M.; Niidomea, T. Optimized polymer coating for magnesium alloy-based bioresorbable scaffolds for long-lasting drug release and corrosion resistance. *Colloids Surf. B: Biointerfaces* **2018**, *163*, 100-106.
13. Ubaid, F.; Radwan, A.B.; Naeem, N.; Shakoor, R.A.; Ahmad, Z.; Montemor, M.F.; Kahraman, R.; Abdullah, A.M.; Soliman, A. Multifunctional self-healing polymeric nanocomposite coatings for corrosion inhibition of steel. *Surf. Coat. Tech.* **2019**, *372*, 121-133.
14. Pulikkalparambil, H.; Siengchin, S.; Parameswaranpillai, J. Corrosion protective self-healing epoxy resin coatings based on inhibitor and polymeric healing agents encapsulated in organic and inorganic micro and nanocontainers. *Nano-Struct. Nano-Obj.* **2018**, *16*, 381-395.

15. Yabuki, A.; Tanabe, S.; Fathona, I.W. Self-healing polymer coating with the microfibers of superabsorbent polymers provides corrosion inhibition in carbon steel. *Surf. Coat. Tech.* **2018**, *341*, 71-77.
16. Singh, A.; Soni, N.; Deyuan, Y.; Kumar, A. A combined electrochemical and theoretical analysis of environmentally benign polymer for corrosion protection of N80 steel in sweet corrosive environment. *Results Phys.* **2019**, *13*, 102116.
17. Achary, G.; Naik, Y.A.; Kumar, S.V.; Venkatesha, T.V.; Sherigara, B.S. An electroactive co-polymer as corrosion inhibitor for steel in sulphuric acid medium. *Appl. Surf. Sci.* **2008**, *254*, 5569-5573.
18. Gopi, D.; Karthikeyan, P.; Kavitha, L.; Surendiran, M. Development of poly(3,4-ethylenedioxythiophene-co-indole-5-carboxylic acid) co-polymer coatings on passivated low-nickelstainless steel for enhanced corrosion resistance in the sulphuric acid medium. *Appl. Surf. Sci.* **2015**, *357*, 122-130.
19. Lin, Y.; Singh, A.; Ebenso, E.E.; Wu, Y.; Zhu, C.; Zhu, M. Effect of poly(methyl methacrylate-co-N-vinyl-2-pyrrolidone) polymer on J55 steel corrosion in 3.5% NaCl solution saturated with CO_2. *J. Taiwan Inst. Chem. E.* **2015**, *46*, 214-222.
20. Mathew, A.M.; Predeep, P. Styrene butadiene co-polymer based conducting polymer composite as an effective corrosion protective coating. *Prog. Org. Coat.* **2012**, *74*, 14-18.
21. Sambyal, P.; Ruhi, G.; Dhawan, R.; Dhawan, S.K. Designing of smart coatings of conducting polymer poly(aniline-co-phenetidine)/SiO2 composites for corrosion protection in marine environment. *Surf. Coat. Tech.* **2016**, *303*, 362-371.
22. Bustos-Terrones, V.; Serratos, I.N.; Castañeda-Villa, N.; Escobar, J.O.V.; Romo, M.A.R.; Córdoba, G.; Chavarín, J.U.; Campos, C.M.; Schulz, J.M.E.; Ortiz, A.D. Functionalized coatings based on organic polymer matrix against the process of corrosion of mild steel in neutral medium. *Prog. Org. Coat.* **2018**, *119*, 221-229.
23. Kaur, H.; Sharma, J.; Jindal, D.; Arya, R.K.; Ahuja, S.K.; Arya, S.B. Crosslinked polymer doped binary coatings for corrosion protection. *Prog. Org. Coat.* **2018**, *125*, 32-39.
24. Azzam, E.M.S.; El-Salam, H.M.A.; Mohamed, R.A.; Shaban, S.M.; Shokry, A. Control the corrosion of mild steel using synthesized polymers based on polyacrylamide. *Egypt. J. Pet.* **2018**, *27*, 897-910.
25. Biswas, A.; Pal, S.; Udayabhanu, G. Experimental and theoretical studies of xanthan gum and its graft co-polymer as corrosion inhibitor for mild steel in 15% HCl. *Appl. Surf. Sci.* **2015**, *353*, 173-183.
26. Madhankumar, A.; Rajendran, N. A promising copolymer of p-phenylendiamine and o-aminophenol: Chemical and electrochemical synthesis, characterization and its corrosion protection aspect on mild steel. *Synth. Met.* **2012**, *162*, 176-185.
27. Aly, K.I.; Younis, O.; Mahross, M.H.; Orabi, E.A.; Hakim, M.A.; Tsutsumi, O.; Mohamed, M.G.; Sayed, M.M. Conducting copolymers nanocomposite coatings with aggregation controlled luminescence and efficient corrosion inhibition properties. *Prog. Org. Coat.* **2019**, *135*, 525-535.
28. Farahati, R.; Ghaffarinejad, A.; Rezania, H.J.; Mousavi-Khoshdel, S.M.; Behzadi, H. Sulfonated aromatic polyamide as water-soluble polymeric corrosion inhibitor of copper in HCl. *Colloids Surf. A.* **2019**, *578*, 123626.
29. Mouaden, K.E.; Ibrahimi, B.E.; Oukhrib, R.; Bazzi, L.; Hammouti, B.; Jbara, O.; Tara, A.; Chauhan, D.S.; Quraishi, M.A. Chitosan polymer as a green corrosion inhibitor for copper in sulfide-containing synthetic seawater. *Int. J. Biol. Macromol.* **2018**, *119*, 1311-1323.

30. Bertuola, M.; Grillo, C.A.; Pissinis, D.E.; Prieto, E.D.; Lorenzo de Mele, M.F. Is the biocompatibility of copper with polymerized natural coating dependent on the potential selected for the electropolymerization process?. *Colloids Surf. B: Biointerfaces* **2017**, *159*, 673-683.

31. Bai, Y.; Chen, Y.; Wang, Q.; Wang, T. Poly(vinyl butyral) based polymer networks with dual-responsive shape memory and self-healing properties. *J. Mater. Chem. A.* **2014**, *2*, 9169-9177.

32. Kumar, P.; Khan, N.; Kumar, D. Polyvinyl butyral (PVB), versetile template for designing nanocomposite/composite materials: A review. *Green Chem. Tech. Letters* **2016**, *2*, 185-194.

33. Jiang, Z.C.; Xiao, Y.Y.; Kang, Y.; Pan, M.; Li, B.J.; Zhang, S. Shape memory polymers based on supramolecular interactions. *ACS Appl. Mater. Interfaces* **2017**, *9*, 20276−20293.

34. Chen, H.M.; Wang, L.; Zhou, S.B. Recent progress in shape memory polymers for biomedical applications. *Chinese J. Polym. Sci.* **2018**, *36*, 905–917.

35. Samide, A.; Bratulescu, G.; Merisanu, C.; Cioatera, N. Anticorrosive coating based on poly(vinyl acetate) formed by electropolymerization on the copper surface. *J. App. Polym. Sci.* **2019**, *136*, 47320.

36. Samide, A.; Ilea, P.; Vladu, A.C. Metronidazole Performance as Corrosion Inhibitor for Carbon Steel, 304L Stainless Steel and Aluminum in Hydrochloric Acid Solution. *Int. J. Electrochem. Sci.* **2017**, *12*, 5964-5983.

37. Samide, A.; Iacobescu, G.E.; Tutunaru, B.; Grecu, R.; Tigae, C.; Spînu, C. Inhibitory Properties of Neomycin Thin Film Formed on Carbon Steel in Sulfuric Acid Solution: Electrochemical and AFM Investigation. *Coatings* **2017**, *7*, 181.

38. Samide, A.; Grecu, R.; Tutunaru, B.; Tigae, C.; Spînu, C. Cisplatin-chemotherapeutic Drug Interactions with the Surface of Some Metal Bioimplants in Physiological Serum. *Int. J. Electrochem. Sci.* **2017**, *12*, 11316-11329.

39. Samide, A.; Stoean, R.; Stoean, C.; Tutunaru, B.; Grecu, R.; Cioatera, N. Investigation of Polymer Coatings Formed by Polyvinyl Alcohol and Silver Nanoparticles on Copper Surface in Acid Medium by Means of Deep Convolutional Neural Networks. *Coatings* **2019**, *9*, 105.

40. Samide, A.; Iacobescu, G.E.; Tutunaru, B.; Tigae, C. Electrochemical and AFM Study of Inhibitory Properties of Thin Film Formed by Tartrazine Food Additive on 304L Stainless Steel in Saline Solution. *Int. J. Electrochem. Sci.* **2017**, *12*, 2088-2101.

41. Grecu, R.; Samide, A.; Iacobescu, G.E.; Cioateră, N.; Popescu, A. Copper Corrosion Inhibitors Based on Polyvinyl alcohol and Silver nanoparticles. *Chem. Ind. Chem. Eng. Q.* **2019**, *25*, 267-275.

42. Carrot, C.; Bendaoud, A.; Pillon, C. Chapter 3. Polyvinyl Butyral in book: *Handbook of Thermoplastics*, CRC Press, 22 Dec 2015, pp. 128.

43. Jiang, X.; Parmeter, J.E.; Estrada, C.A.; Wayne Goodman, D. The adsorption and decomposition of methanol on copper on the Rh(100) surface. *Surf. Sci.* **1991**, *249*, 44-60.